

On Number of Almost Blank Subframes in Heterogeneous Cellular Networks

Michal Čiřny, *Student Member, IEEE*, Haining Wang, Risto Wichman,
Zhi Ding, *Fellow, IEEE*, Carl Wijting, *Senior Member, IEEE*

Abstract

In heterogeneous cellular scenarios with macrocells, femtocells or picocells users may suffer from significant co-channel cross-tier interference. To manage this interference 3GPP introduced almost blank subframe (ABSF), a subframe in which the interferer tier is not allowed to transmit data. Vulnerable users thus get a chance to be scheduled in ABSFs with reduced cross-tier interference. We analyze downlink scenarios using stochastic geometry and formulate a condition for the required number of ABSFs based on base station placement statistics and user throughput requirement. The result is a semi-analytical formula that serves as a good initial estimate and offers an easy way to analyze impact of network parameters. We show that while in macro/femto scenario the residue ABSF interference can be well managed, in macro/pico scenario it affects the number of required ABSFs strongly. The effect of ABSFs is subsequently demonstrated via user throughput simulations. Especially in the macro/pico scenario, we find that using ABSFs is advantageous for the system since victim users no longer suffer from poor performance for the price of relatively small drop in higher throughput percentiles.

Index Terms

Almost blank subframe, interference management, heterogeneous network, HetNet;

Manuscript created November 9, 2012; revised April 7 and July 17, 2013; accepted July 29, 2013. This work was supported by Academy of Finland, National Science Foundation grants 1147930 and 1321143, TEKES, Graduate School in Electronics, Telecommunications and Automation (GETA) and HPY Foundation.

M. Čiřny and R. Wichman are with Department of Signal Processing and Acoustics, Aalto University School of Electrical Engineering, 00076 Aalto, Finland (e-mail: {michal.ciřny, risto.wichman}@aalto.fi).

H. Wang and Z. Ding are with Department of Electrical and Computer Engineering, University of California, Davis, California 95616 (e-mail: {hnlwang, zding}@ucdavis.edu).

C. Wijting is with Nokia Research Center in Otaniemi, Otaniementie 19, 02150 Espoo, Finland (e-mail: carl.wijting@nokia.com).

I. INTRODUCTION

Almost blank subframes (ABSFs) are part of Enhanced Inter-Cell Interference Coordination (eICIC) framework [1] that the 3GPP members have proposed [2] as means to combat excessive co-channel cross-tier interference in heterogeneous network (HetNet) scenarios. HetNet scenarios are generally cellular network scenarios that cover different types of low-power nodes, such as base stations (BSs), relays or remote radio heads, as underlay to the traditional macrocell tier. HetNet scenarios that are specifically targeted to benefit from ABSFs are combinations of macrocells with closed access femtocells (macro/femto) and macrocells with open access picocells (macro/pico) [3].

Femto base station (FBS), also called Home eNodeB (HeNB), is a low-power BS that is deployable by the end user and connects to the core network of a cellular operator by means of wired broadband connection. In the eyes of the operator this is a win-win situation as the users (femto user equipments, FUEs) benefit from higher connection throughput while the use of commonly available wired broadband (such as e.g. digital subscriber line) decreases costs of expanding network infrastructure. In a closed access femtocell only selected users have access to the FBS services, creating thus a closed subscriber group (CSG). A drawback of this is that a non-member macro UE (MUE) that is located close to a closed access FBS can suffer from excessive interference. Proposed (non-ABSF) solutions for downlink interference management in OFDMA femtocells include for example FBS power control [4], frequency partitioning [5], [6], precoding [7], cognitive radio approach [8] and augmentation of scheduling algorithms [9].

Pico base station (PBS) is practically a normal base station with lower transmit power and therefore smaller coverage region. The point of PBS deployment lies not in covering areas where macro tier signal is too low, but in augmenting the macro tier in areas where the concentration of MUEs is too high to be efficiently served by a macro base station (MBS). For such augmentation to be successful it has been shown (see [10] for the first suggestion) that even UEs that have somehow stronger signal from the closest MBS should be allowed to associate to a PBS, thus leading to a so-called cell range expansion (CRE) concept. Hence, more UEs will associate with PBSs, leading to more efficient frequency reuse and desirable traffic offloading from the macro tier. However, as the CRE description already suggests, some pico UEs (PUEs) see strong interference from the macro tier. Proposed (non-ABSF) solutions for downlink interference management in the macro/pico scenario include interference cancellation

[11], frequency partitioning [12] and MBS power control [13].

The ABSF concept is based on blanking some subframes of the interferer tier and scheduling the especially vulnerable UEs in these subframes. The vulnerable users thus get part of radio resources where cross-tier interference is lower. The ABSFs are called almost blank because not all resource elements are allowed to be blanked - the cell-specific reference symbols (CRS) that are used for radio resource management (RRM) measurements and channel estimation have to remain present. The strong interference in CRS resource elements is a separate issue and was suggested to be tackled by interference cancellation (see [14] or [15] also for other control channel challenges), but such considerations are out of scope of this work. Alternatively to ABSF, the BS can configure an empty MBSFN (Multicast-Broadcast Single Frequency Network) subframe, but its use is more constrained, therefore, our focus will be on the ABSF. Compared to other mentioned interference management solutions, the ABSF concept is simple enough to be incorporated into often technically entangled 3GPP specifications and at the same time it has found rather wide acceptance among the standardization partners.

The interferer tier in the macro/femto scenario is the femto tier, while in the macro/pico scenario it is the macro tier. In case there are both FBSs and PBSs within MBS coverage, there might be need for ABSFs in femto tier as well as in macro tier. As the (significant) cross-tier interference can come from multiple BSs, the amount and position of ABSFs has to be coordinated within the network. Indeed, the organization of ABSFs is planned as a part of self organizing network (SON) concept [16]. In our work we will propose how the number of ABSFs for downlink interference management can be set globally based on BS placement statistics. Such relationship can then serve as an initial estimate or as a backup solution when the distributed coordination does not serve its purpose. We will derive the necessary number of ABSFs for macro/femto and macro/pico scenarios separately and, if needed, the results can be easily combined.

To our best knowledge the question of deriving the number of necessary ABSFs has not been addressed before this work. Besides the mentioned concept research [3], [15] the work is quite sparse. For the macro/femto scenario, some simulation results of using ABSFs have been published in [17] and [18]. In [19] the authors introduce a coordination framework for ABSFs, including channel quality indication (CQI) processing, and suggest control messages that are needed for such operation. Simulated performance of the macro/pico scenario has been shown in [20], while [21] presents also analytical insight into the topic. During the second round of the

review process of our work, a solid article on the topic has become available [22]. The authors use similar model as we do and derive a rate coverage of the system. They do not however consider residue interference in the ABSF.

We address the problem by setting the number of ABSFs globally using tools from stochastic geometry [23], [24]. Base stations and users are modeled as 2D stochastic processes and spatial relation between a user and its closest interferer is leveraged to define victim users, i.e., users that require interference management. Parametrization of the stochastic models and properties of the victim users are then used to formulate the number of necessary ABSFs. We thus give a semi-closed form connection between the stochastic intensity and other parameters and the minimum number of subframes that can be quickly used to determine the fraction of radio resources needed for interference management. Subsequently, we analyze dependence on individual model parameters, the most important result from which is that in macro/pico scenario the residue ABSF interference has a strong effect on the required number of ABSFs. Finally, we demonstrate the effect of derived number of ABSFs on user throughput via simulations. The results show moderate performance gain for victim users in macro/femto scenario, but in macro/pico scenario the improvement is substantial.

The remainder of the paper is structured as follows: Section II introduces the stochastic geometry-based system model and defines victim UEs. In Section III we derive the success probability of victim UEs, i.e., probability that signal-to-interference ratio (SIR) is higher than a predefined threshold. In Section IV we use the success probability to set condition for the necessary number of ABSFs. In Section V we evaluate the effect of ABSFs by means of Monte Carlo simulations. Section VI concludes the paper. Most of the sections are divided into two parts, one for macro/femto scenario and one for macro/pico scenario.

II. SYSTEM MODEL

In this work we model BS and UE placements as homogeneous Poisson point processes (PPP). In [25] it has been shown that the random BS placement produces a good lower bound for SINR distribution, a regular grid BS deployment gives an upper bound, and the actual truth lies somewhere in between. In [26] the authors have taken two samples of real world BS placements and shown that PPP is not actually a good model for them, because it lacks interaction between points. Nevertheless, the use of PPP model is prevalent (see e.g. [27] for heterogeneous networks) as it offers a rare analytical insight into a larger scale network.

Radio channel conditions are modeled by a combination of distance dependent path loss $H(r) = r^{-\alpha}$, where α is path loss exponent, and fast Rayleigh fading with exponential power distribution $h \sim \exp(1)$. For the sake of tractability we consider two general simplifications. Firstly, we do not model shadow fading. Although it is possible to include shadow fading in initial model equations, a considerable degree of tractability is lost (see [25] and [28]). Secondly, the residue ABSF interference is considered white. In reality, the victim receiver would see full interference on resource elements where the interferer transmits CRS, and some leakage on other resource elements. However, considering that the CRS position varies between cells and all data is subject to scrambling, the white interference model is not extremely far-fetched.

We note here that although 3GPP specifications and state of the art research work offer quite a few techniques that could supplement the use of ABSF for cross-tier interference management, the scope of this study and structure of the system model does not allow us to consider them. We assume a single antenna transceiver at both BS and UE, hence multi-antenna techniques are not considered. Coordinated multi-point transmission and advanced receiver processing are also out of our scope.

A. Macro/femto scenario

In the first scenario we have an overlay macrocell PPP Θ_{MBS} of intensity λ_{M} and an underlay femtocell PPP Θ_{FBS} of intensity λ_{F} . Macro UEs (MUEs) form another PPP Θ_{MUE} of intensity λ_{MUE} . Because we are interested in protecting MUEs from CSG femtocells, we do not need to model femto UEs. Processes Θ_{MBS} , Θ_{FBS} and Θ_{MUE} are all separate and independent among each other. Indoor/outdoor positions and walls are not considered in the model. MUE is associated to a macro BS (MBS) with the best long-term channel conditions, i.e., the geographically closest one, as in [25]. Transmission powers of MBS and FBS are denoted by P_{M} and P_{F} , respectively. Path loss exponent on MBS-UE links is α_{M} , on FBS-UE links it is α_{F} . Data traffic in macro and femto layer is modeled by base station load values ϕ_{M} and ϕ_{F} , respectively. A comprehensive analysis of load impact on PPP-based model of cellular network has been done in [29]. Although our work uses a different UE-BS association model, the traffic model philosophy remains the same.

Let us now have an MUE that is associated to MBS of distance r_{M} . We say that an FBS is a dominant interferer (DI) to given MUE if the MUE-FBS distance r_{F} is smaller than kr_{M} , where k is a DI-defining coefficient. We then define a victim MUE as an MUE that has one

or more DIs. MUE can measure long term channel conditions (and thus estimate distance) of FBSs by performing a reference-signal-received-power (RSRP) measurement. Presence of DIs (or victim status) is then reported to MBS, which uses the knowledge to decide which MUEs will be scheduled in ABSF and which in normal subframe (NSF).

Value of the DI-defining coefficient k is important here. Its basic purpose is to take into account difference between MBS and FBS transmission powers and path loss exponents and consider the maximum interferer power that the MUE receiver can withstand. If, for example, $\alpha_M = \alpha_F = \alpha$ and the minimum required SIR at MUE is 0dB, $k = (P_F/P_M)^{1/\alpha}$. With $\alpha_M \neq \alpha_F$ the relation between received powers can no longer be transformed to linear relation between r_F and r_M and our condition becomes only approximate.

The definition of victim MUE gives k also another dimension. It might happen that interference from multiple FBSs that are not marked as DIs is unbearable and the given MUE should be marked as victim. A safety margin in k value is an option how to counterweight this issue.

Our definition of DIs via k resembles [30] where a contour of equal power is used to decide how to divide available spectrum. The authors however do not pursue its effect on SIR, nor do they analyze it from statistical point of view.

B. Macro/pico scenario

In the second scenario there is again an overlay macrocell PPP Θ_{MBS} of intensity λ_M and an underlay picocell PPP Θ_{PBS} of intensity λ_P . Macro UEs (MUEs) form again a PPP Θ_{MUE} of intensity λ_{MUE} . Processes Θ_{MBS} , Θ_{PBS} and Θ_{MUE} are separate and independent among each other. As we now have an open access policy, part of the MUEs will actually be associated to PBSs and thus called PUEs. Drawing inspiration from [27], an MUE is associated to a PBS if the distance to the closest PBS r_P is smaller than $k_1 r_M$, where r_M is the distance to the closest MBS. In case there is no PBS within $k_1 r_M$ distance, the MUE is associated to the closest MBS. The k_1 coefficient takes into account differences in MBS and PBS transmission powers P_M and P_P , respectively, and the association bias κ . Unlike [31] that tries to find a framework for κ optimization, we keep the value constant and analyze its effect on the required number of ABSFs. Path loss exponent on MBS-UE links is α_M , on PBS-UE links it is α_P . The MBS and PBS load values are denoted as ϕ_M and ϕ_P , respectively.

The dominant interferers to a PUE are MBSs that fulfill $r_P > k_2 r_M$, where r_P is distance between PUE and the associated PBS, k_2 is the DI-defining coefficient and r_M is distance to

given MBS. With positive association bias we have $k_1 > k_2$. Victim PUEs are PUEs that have one or more DIs. They are thus identified by a pair of inequalities $k_2 r_M < r_P < k_1 r_M$. Presence of DIs (or victim status) are reported from PUE to PBS, which can then use the knowledge to request ABSFs from the macro tier. The k_2 coefficient has the same meaning as k in macro/femto scenario and can as well be used to address the issue of multiple DIs.

III. SUCCESS PROBABILITY

In this section we derive success probabilities of victim MUEs and PUEs in our scenarios, which we then use in Section IV to set the necessary number of ABSFs. We use the name success probability as in [27], i.e., a probability that UE has a signal-to-interference-ratio (SIR) higher than an outage threshold. SIR is used in this work to approximate signal-to-interference-plus-noise-ratio (SINR), as we are modeling interference limited networks. The success probability represents a CCDF of SIR. While for arbitrary located UEs equivalent result have been presented e.g. in [32], [33] and [34], conditioning on presence of dominant interferers has to our best knowledge not been done before.

A. Macro/femto scenario

Signal-to-interference-ratio at a victim MUE on single resource block is given by formula

$$\gamma = \frac{P_M h r_M^{-\alpha_M}}{I_M + \rho_A (I_{DI} + I_F)}, \quad (1)$$

where h denotes fast fading power gain, I_M denotes sum interference power from the macro tier (all MBSs except associated one), I_{DI} denotes sum interference power from DIs, I_F denotes sum interference power from non-DI FBSs and ρ_A denotes residue ABSF interference. Results in this section are derived for ABSF, for NSF one would simply omit ρ_A . Success probability is defined as

$$\mathbb{P} \{ \gamma > \gamma_0 \}, \quad (2)$$

where γ_0 represents the outage threshold.

To increase clarity and give insight on how the work has progressed we first derive success probability in case of full load and single DI present. After that, we generalize it for arbitrary load values and one or more DIs present.

1) *A single dominant interferer*: Probability that the number of FBS DIs $N_{\text{DI}}^{(\text{F})}$ around a randomly chosen MUE equals one is given from the definition of PPP as

$$\mathbb{P} \left\{ N_{\text{DI}}^{(\text{F})} = 1 \mid r_{\text{M}} \right\} = \pi k^2 \lambda_{\text{F}} r_{\text{M}}^2 \exp \left(-\pi k^2 \lambda_{\text{F}} r_{\text{M}}^2 \right). \quad (3)$$

By averaging over r_{M} we get

$$\mathbb{P} \left\{ N_{\text{DI}}^{(\text{F})} = 1 \right\} = \int_{r_{\text{M}}} \mathbb{P} \left\{ N_{\text{DI}}^{(\text{F})} = 1 \mid r \right\} f_{r_{\text{M}}}(r) dr \quad (4)$$

$$\begin{aligned} &= \int_0^{\infty} \mathbb{P} \left\{ N_{\text{DI}}^{(\text{F})} \mid r \right\} 2\pi \lambda_{\text{M}} r \\ &\quad \times \exp \left(-\pi \lambda_{\text{M}} r^2 \right) dr \end{aligned} \quad (5)$$

$$= \frac{k^2 \lambda_{\text{F}} \lambda_{\text{M}}}{(k^2 \lambda_{\text{F}} + \lambda_{\text{M}})^2}. \quad (6)$$

CDF of r_{M} conditioned on 1 FBS within kr_{M} is then

$$F_{r_{\text{M}}|k}^{(1)}(R) = \mathbb{P} \left\{ r_{\text{M}} \leq R \mid N_{\text{DI}}^{(\text{F})} = 1 \right\} \quad (7)$$

$$= \frac{\mathbb{P} \left\{ r_{\text{M}} \leq R, N_{\text{DI}}^{(\text{F})} = 1 \right\}}{\mathbb{P} \left\{ N_{\text{DI}}^{(\text{F})} = 1 \right\}} \quad (8)$$

$$= \frac{\int_0^R \mathbb{P} \left\{ N_{\text{DI}}^{(\text{F})} = 1 \mid r_{\text{M}} = r \right\} f_{r_{\text{M}}}(r) dr}{\frac{k^2 \lambda_{\text{F}} \lambda_{\text{M}}}{(k^2 \lambda_{\text{F}} + \lambda_{\text{M}})^2}} \quad (9)$$

$$\begin{aligned} &= \frac{(k^2 \lambda_{\text{F}} + \lambda_{\text{M}})^2}{k^2 \lambda_{\text{F}} \lambda_{\text{M}}} \int_0^R \mathbb{P} \left\{ N_{\text{DI}}^{(\text{F})} = 1 \mid r_{\text{M}} = r \right\} \\ &\quad \times 2\pi \lambda_{\text{M}} r \exp \left(-\pi \lambda_{\text{M}} r^2 \right) dr \end{aligned} \quad (10)$$

$$\begin{aligned} &= 1 - \left(1 + \pi (k^2 \lambda_{\text{F}} + \lambda_{\text{M}}) R^2 \right) \\ &\quad \times \exp \left(-\pi (k^2 \lambda_{\text{F}} + \lambda_{\text{M}}) R^2 \right). \end{aligned} \quad (11)$$

By differentiation we get a PDF

$$f_{r_{\text{M}}|k}^{(1)}(r) = 2\pi^2 (k^2 \lambda_{\text{F}} + \lambda_{\text{M}})^2 r^3 \exp \left(-\pi (k^2 \lambda_{\text{F}} + \lambda_{\text{M}}) r^2 \right). \quad (12)$$

The success probability of a victim MUE is

$$\begin{aligned}
& \mathbb{P} \left\{ \gamma > \gamma_0 \mid N_{\text{DI}}^{(\text{F})} = 1 \right\} \\
&= \mathbb{E}_{I, r_M}^{(1)} \left\{ \mathbb{P} \left\{ \frac{P_M h r_M^{-\alpha_M}}{I_M + \rho_A (I_{\text{DI}} + I_{\text{F}})} > \gamma_0 \right\} \right\} \\
&= \int_0^\infty \mathbb{E}_I^{(1)} \left\{ \mathbb{P} \left\{ \frac{P_M h r^{-\alpha_M}}{I_M + \rho_A (I_{\text{DI}} + I_{\text{F}})} > \gamma_0 \right\} \right\} \\
&\quad \times f_{r_M|k}^{(1)}(r) dr.
\end{aligned} \tag{13}$$

The reader may notice that on RHS of (13) we have omitted the condition $N_{\text{DI}}^{(\text{F})} = 1$. This is purely for space purposes and we will repeat it a few times throughout the paper. The inner probability from (13) can be found as

$$\mathbb{E}_I^{(1)} \{ \} = \mathbb{E}_I^{(1)} \left\{ \mathbb{P} \left\{ \frac{P_M h r^{-\alpha_M}}{I_M + \rho_A (I_{\text{DI}} + I_{\text{F}})} > \gamma_0 \right\} \right\} \tag{14}$$

$$= \mathbb{E}_I^{(1)} \left\{ \mathbb{P} \left\{ h > \frac{\gamma_0 (I_M + \rho_A (I_{\text{DI}} + I_{\text{F}}))}{P_M r^{-\alpha_M}} \right\} \right\} \tag{15}$$

$$= \mathbb{E}_I^{(1)} \left\{ \exp \left(-\frac{\gamma_0 r^{\alpha_M}}{P_M} (I_M + \rho_A I_{\text{DI}} + \rho_A I_{\text{F}}) \right) \right\} \tag{16}$$

$$\begin{aligned}
&= \mathbb{E}_{I_M}^{(1)} \left\{ \exp \left(-\frac{\gamma_0 r^{\alpha_M}}{P_M} I_M \right) \right\} \mathbb{E}_{I_{\text{DI}}}^{(1)} \left\{ \exp \left(-\frac{\gamma_0 r^{\alpha_M}}{P_M} \rho_A I_{\text{DI}} \right) \right\} \\
&\quad \times \mathbb{E}_{I_{\text{F}}}^{(1)} \left\{ \exp \left(-\frac{\gamma_0 r^{\alpha_M}}{P_M} \rho_A I_{\text{F}} \right) \right\}.
\end{aligned} \tag{17}$$

The first and the last terms in (17) have been derived in [25] and are given by

$$\mathbb{E}_{I_M}^{(1)} \{ \} = \exp \left(-\pi \lambda_M r^2 \rho(\gamma_0, \alpha_M) \right) \tag{18}$$

and

$$\mathbb{E}_{I_{\text{F}}}^{(1)} \{ \} = \exp \left(-\pi k^2 \lambda_{\text{F}} r^2 \rho \left(\frac{\gamma_0 \rho_A P_{\text{F}} r^{\alpha_M}}{k^{\alpha_{\text{F}}} P_{\text{M}} r^{\alpha_{\text{F}}}}, \alpha_{\text{F}} \right) \right), \tag{19}$$

where

$$\rho(\gamma, \alpha) = \int_{\gamma^{-\frac{2}{\alpha}}}^\infty \frac{\gamma^{\frac{2}{\alpha}}}{1 + u^{\frac{\alpha}{2}}} du. \tag{20}$$

For averaging the dominant interference term in (17) we exploit the Laplace transform of exponential function as given here

$$\begin{aligned} & \mathbb{E}_{I_{\text{DI}}}^{(1)} \{ \exp(-s I_{\text{DI}}) \} \\ &= \mathbb{E}_{I_{\text{DI}}}^{(1)} \{ \exp(-s P_{\text{F}} h_{\text{DI}} r_{\text{DI}}^{-\alpha_{\text{F}}}) \} \end{aligned} \quad (21)$$

$$= \mathbb{E}_{r_{\text{DI}}}^{(1)} \left\{ \frac{1}{1 + s P_{\text{F}} r_{\text{DI}}^{-\alpha_{\text{F}}}} \right\} \quad (22)$$

$$= \int_{r_{\text{DI}}} \frac{1}{1 + s P_{\text{F}} u^{-\alpha_{\text{F}}}} f_{r_{\text{DI}}}(u) du \quad (23)$$

$$= \int_0^{kr} \frac{1}{1 + s P_{\text{F}} u^{-\alpha_{\text{F}}}} \frac{2u}{(kr)^2} du \quad (24)$$

$$= 1 - {}_2F_1 \left(1, \frac{2}{\alpha_{\text{F}}}, \frac{2+\alpha_{\text{F}}}{\alpha_{\text{F}}}, -\frac{(kr)^{\alpha_{\text{F}}}}{s P_{\text{F}}} \right), \quad (25)$$

where h_{DI} and r_{DI} are fast fading power and link distance between victim MUE and DI FBS, respectively, and ${}_2F_1(\cdot)$ is the hypergeometric function. For $s = \frac{\gamma_0 r^{\alpha_{\text{M}}} \rho_{\text{A}}}{P_{\text{M}}}$ this gives

$$\begin{aligned} & \mathbb{E}_{I_{\text{DI}}}^{(1)} \left\{ \exp \left(-\frac{\gamma_0 r^{\alpha_{\text{M}}}}{P_{\text{M}}} \rho_{\text{A}} I_{\text{DI}} \right) \right\} \\ &= 1 - {}_2F_1 \left(1, \frac{2}{\alpha_{\text{F}}}, \frac{2+\alpha_{\text{F}}}{\alpha_{\text{F}}}, -\frac{k^{\alpha_{\text{F}}} P_{\text{M}} r^{\alpha_{\text{F}}}}{\gamma_0 \rho_{\text{A}} P_{\text{F}} r^{\alpha_{\text{M}}}} \right). \end{aligned} \quad (26)$$

The PDF of r_{M} (12) and interference terms (18), (19) and (26) can now be plugged into (13). In case of single path loss exponent $\alpha_{\text{M}} = \alpha_{\text{F}} = \alpha$ the integration variable disappears from inside the $\rho(\cdot)$ and ${}_2F_1(\cdot)$ functions and we get a closed form solution

$$\begin{aligned} & \mathbb{P} \left\{ \gamma > \gamma_0 \mid N_{\text{DI}}^{(\text{F})} = 1, \alpha_{\text{M}} = \alpha_{\text{F}} = \alpha \right\} \\ &= \frac{(k^2 \lambda_{\text{F}} + \lambda_{\text{M}})^2 \left(1 - {}_2F_1 \left(1, \frac{2}{\alpha}, \frac{2+\alpha}{\alpha}, -\frac{k^{\alpha} P_{\text{M}}}{\gamma_0 \rho_{\text{A}} P_{\text{F}}} \right) \right)}{\left(\lambda_{\text{M}} [1 + \rho(\gamma_0, \alpha)] + k^2 \lambda_{\text{F}} \left[1 + \rho \left(\frac{\gamma_0 \rho_{\text{A}} P_{\text{F}}}{k^{\alpha} P_{\text{M}}}, \alpha \right) \right] \right)^2}. \end{aligned} \quad (27)$$

2) *One or more dominant interferers:* A probability that an MUE has one or more FBS dominant interferers within kr_{M} distance is complementary to probability that there are no FBSs within that distance. Using the same approach as with the single DI we get the probability

$$\mathbb{P} \left\{ N_{\text{DI}}^{(\text{F})} \geq 1 \right\} = \frac{k^2 \lambda_{\text{F}}}{k^2 \lambda_{\text{F}} + \lambda_{\text{M}}} \quad (28)$$

and the PDF of distance from closest MBS

$$f_{r_M|k}(r) = \frac{k^2 \lambda_F + \lambda_M}{k^2 \lambda_F} 2\pi \lambda_M r \times \left(\exp(-\pi \lambda_M r^2) - \exp(-\pi (k^2 \lambda_F + \lambda_M) r^2) \right). \quad (29)$$

The success probability is again given by

$$\begin{aligned} \mathbb{P} \left\{ \gamma > \gamma_0 \mid N_{\text{DI}}^{(\text{F})} \geq 1 \right\} \\ = \int_0^\infty \mathbb{E}_I \left\{ \mathbb{P} \left\{ \frac{P_M h r^{-\alpha_M}}{I_M + \rho_A (I_{\text{DI}} + I_F)} > \gamma_0 \right\} \right\} f_{r_M|k}(r) dr \end{aligned} \quad (30)$$

and the inner probability by

$$\begin{aligned} \mathbb{E}_I \{ \} &= \mathbb{E}_{I_M} \left\{ \exp \left(-\frac{\gamma_0 r^{\alpha_M}}{P_M} I_M \right) \right\} \\ &\times \mathbb{E}_{I_{\text{DI}}} \left\{ \exp \left(-\frac{\gamma_0 r^{\alpha_M}}{P_M} \rho_A I_{\text{DI}} \right) \right\} \\ &\times \mathbb{E}_{I_F} \left\{ \exp \left(-\frac{\gamma_0 r^{\alpha_M}}{P_M} \rho_A I_F \right) \right\}. \end{aligned} \quad (31)$$

The I_M and I_F terms generalized for arbitrary BS load values are given here:

$$\mathbb{E}_{I_M} \{ \} = \exp \left(-\pi \phi_M \lambda_M r^2 \rho (\gamma_0, \alpha_M) \right) \quad (32)$$

$$\mathbb{E}_{I_F} \{ \} = \exp \left(-\pi \phi_F k^2 \lambda_F r^2 \rho \left(\frac{\gamma_0 \rho_A P_F r^{\alpha_M}}{k^{\alpha_F} P_M r^{\alpha_F}}, \alpha_F \right) \right) \quad (33)$$

To derive $\mathbb{E}_{I_{\text{DI}}} \{ \}$ we will use $\mathbb{E}_{I_{\text{DI}}}^{(1)} \{ \}$ from (26). We denote $I_{\text{DI}} = \sum_{i=1}^{N_{\text{DI}}^{(\text{F})}} I_{\text{DI}}^{(i)}$, where $N_{\text{DI}}^{(\text{F})}$ is a random variable describing the number of FBS DIs within kr conditioned on presence of at least one. With full load we can get an exact expression

$$\mathbb{E}_{I_{\text{DI}}} \{ \} = \mathbb{E} \left\{ \prod_{i=1}^{N_{\text{DI}}^{(\text{F})}} \mathbb{E} \left[\exp \left(-\frac{\gamma_0 r^{\alpha_M}}{P_M} \rho_A I_{\text{DI}}^{(i)} \right) \right] \middle| N_{\text{DI}}^{(\text{F})} \right\} \quad (34)$$

$$= \mathbb{E} \left\{ \mathbb{E}_{I_{\text{DI}}}^{(1)} \{ \}^{N_{\text{DI}}^{(\text{F})}} \right\} \quad (35)$$

$$= \text{PGF}_{N_{\text{DI}}^{(\text{F})}} \left(\mathbb{E}_{I_{\text{DI}}}^{(1)} \{ \} \right), \quad (36)$$

where $\text{PGF}_{N_{DI}^{(F)}}$ is the probability generation function of $N_{DI}^{(F)}$ given by

$$\text{PGF}_{N_{DI}^{(F)}}(x) = \sum_{i=1}^{\infty} x^i f_{N_{DI}^{(F)}}(i) \quad (37)$$

$$= \sum_{i=1}^{\infty} x^i \frac{(\pi k^2 \lambda_F r^2)^i \exp(-\pi k^2 \lambda_F r^2)}{1 - \exp(-\pi k^2 \lambda_F r^2)} \quad (38)$$

$$= \frac{\exp(x\pi k^2 \lambda_F r^2) - 1}{\exp(\pi k^2 \lambda_F r^2) - 1} \quad (39)$$

where $f_{N_{DI}^{(F)}}(n)$ is the PMF of $N_{DI}^{(F)}$. With a general load ϕ_F , the expression does not hold. In that case we can use a good approximation

$$\begin{aligned} \mathbb{E}_{I_{DI}} \{ \} &\approx \mathbb{E}_{I_{DI}}^{(1)} \{ \}^{\phi_F \bar{N}_{DI}^{(F)}} \\ &= \left[1 - {}_2F_1 \left(1, \frac{2}{\alpha_F}, \frac{2+\alpha_F}{\alpha_F}, -\frac{k_F^\alpha P_M r^{\alpha_F}}{\gamma_0 \rho_A P_F r^{\alpha_M}} \right) \right]^{\phi_F \bar{N}_{DI}^{(F)}}, \end{aligned} \quad (40)$$

where $\bar{N}_{DI}^{(F)}$ is the mean value of $N_{DI}^{(F)}$ given by

$$\bar{N}_{DI}^{(F)} = \frac{\pi k^2 \lambda_F r^2}{1 - \exp(-\pi k^2 \lambda_F r^2)}. \quad (41)$$

The interference terms can now be put into (30) to calculate the success probability. Unlike (27), the integral in (30) cannot be simplified into a more digestible form even with single path loss exponent and has to be evaluated numerically.

B. Macro/pico scenario

In the second scenario, the downlink signal-to-interference-ratio at a victim PUE is defined as

$$\gamma = \frac{P_P h r_P^{-\alpha_P}}{I_P + \rho_A (I_{DI} + I_M)}, \quad (42)$$

where I_P is sum interference power from the pico tier (all PBSs except associated one), I_{DI} is sum interference power from dominant MBS interferers and I_M is sum interference power from all other MBS interferers. In the rest of the subsection we will state the most important results for the success probability. Derivation follows the same logic as in the first scenario.

The probability that a UE is actually a victim PUE is

$$\mathbb{P} \{ k_2 r_M < r_P < k_1 r_M \} = \frac{\lambda_M}{\lambda_M + k_2^2 \lambda_P} - \frac{\lambda_M}{\lambda_M + k_1^2 \lambda_P} \quad (43)$$

and the PDF of r_P of a victim PUE

$$f_{r_P|k}(r) = 2\pi r \frac{(\lambda_M + k_1^2 \lambda_P)(\lambda_M + k_2^2 \lambda_P)}{(k_1^2 - k_2^2) \lambda_M} \times \left[\exp\left(-\pi \left(\frac{\lambda_M}{k_1^2} + \lambda_P\right) r^2\right) - \exp\left(-\pi \left(\frac{\lambda_M}{k_2^2} + \lambda_P\right) r^2\right) \right]. \quad (44)$$

The success probability is given by integral

$$\begin{aligned} & \mathbb{P}\{\gamma > \gamma_0 | k_2 r_M < r_P < k_1 r_M\} \\ &= \int_0^\infty \mathbb{E}_I \left\{ \mathbb{P} \left\{ \frac{P_P h r^{-\alpha_P}}{I_P + \rho_A (I_{DI} + I_M)} > \gamma_0 \right\} \right\} \\ & \quad \times f_{r_P|k}(r) dr \end{aligned} \quad (45)$$

with the inner probability

$$\begin{aligned} \mathbb{E}_I \{\} &= \mathbb{E}_{I_P} \left\{ \exp\left(-\frac{\gamma_0 r^{\alpha_P}}{P_P} I_P\right) \right\} \\ & \quad \times \mathbb{E}_{I_{DI}} \left\{ \exp\left(-\frac{\gamma_0 r^{\alpha_P}}{P_P} \rho_A I_{DI}\right) \right\} \\ & \quad \times \mathbb{E}_{I_M} \left\{ \exp\left(-\frac{\gamma_0 r^{\alpha_P}}{P_P} \rho_A I_M\right) \right\}. \end{aligned} \quad (46)$$

The non-dominant interference terms \mathbb{E}_{I_P} and \mathbb{E}_{I_M} are given here:

$$\mathbb{E}_{I_P} \{\} = \exp\left(-\pi \phi_P \lambda_P r^2 \rho(\gamma_0, \alpha_P)\right) \quad (47)$$

$$\mathbb{E}_{I_M} \{\} = \exp\left(-\pi \phi_M \frac{\lambda_M}{k_2^2} r^2 \rho\left(\frac{\gamma_0 k_2^{\alpha_M} \rho_A P_M r^{\alpha_P}}{P_P r^{\alpha_M}}, \alpha_M\right)\right) \quad (48)$$

Fully loaded dominant interference term can be calculated using

$$\mathbb{E}_{I_{DI}} \{\} = \frac{\exp\left(\mathbb{E}_{I_{DI}}^{(1)} \{\} \pi \left(\frac{1}{k_2^2} - \frac{1}{k_1^2}\right) \lambda_M r^2\right) - 1}{\exp\left(\pi \left(\frac{1}{k_2^2} - \frac{1}{k_1^2}\right) \lambda_M r^2\right) - 1} \quad (49)$$

where

$$\begin{aligned} \mathbb{E}_{I_{DI}}^{(1)} \{\} &= \left(\frac{k_1 k_2}{k_1^2 - k_2^2} \right. \\ & \quad \times \left[\frac{1}{k_2^2} {}_2F_1\left(1, -\frac{2}{\alpha_M}, \frac{\alpha_M - 2}{\alpha_M}, \frac{-\gamma_0 k_2^{\alpha_M} \rho_A P_M r^{\alpha_P}}{P_P r^{\alpha_M}}\right) \right. \\ & \quad \left. \left. - \frac{1}{k_1^2} {}_2F_1\left(1, -\frac{2}{\alpha_M}, \frac{\alpha_M - 2}{\alpha_M}, \frac{-\gamma_0 k_1^{\alpha_M} \rho_A P_M r^{\alpha_P}}{P_P r^{\alpha_M}}\right) \right] \right). \end{aligned} \quad (50)$$

For a general load ϕ_M we then have

$$\mathbb{E}_{I_{DI}} \{ \} \approx \mathbb{E}_{I_{DI}}^{(1)} \{ \}^{\phi_M \bar{N}_{DI}^{(M)}}, \quad (51)$$

where $\bar{N}_{DI}^{(M)}$ is the average number of MBS DIs calculated as

$$\bar{N}_{DI}^{(M)} = \frac{\pi \lambda_M \left(\frac{1}{k_2^2} - \frac{1}{k_1^2} \right) r^2}{1 - \exp \left(-\pi \lambda_M \left(\frac{1}{k_2^2} - \frac{1}{k_1^2} \right) r^2 \right)} \quad (52)$$

Like in the first scenario, even with single path loss exponent the final integral (45) can be evaluated only numerically.

IV. NUMBER OF ABSFs

3GPP is introducing ABSFs to protect victim UEs. In both considered scenarios, victim UEs as we defined them are easily identified by presence of dominant interferers in the vicinity based on RSRP measurements. We can thus focus all our attention on the victim UEs and avoid a general and complicated sum rate optimization problem with a simplified one

$$\begin{aligned} & \underset{N_A}{\text{maximize}} && C_{NV}(N_A) \\ & \text{subject to} && C_V(N_A) \geq C_{V,\min}, \\ & && 0 \leq N_A \leq N_S, \end{aligned} \quad (53)$$

where N_S represents number of subframes in a frame, N_A represents number of ABSFs in a frame, C_{NV} stands for throughput of non-victim UEs, C_V stands for victim UE throughput and $C_{V,\min}$ stands for the minimum required victim UE throughput, a parameter of choice. We will not define $C_{NV}(N_A)$ more closely because any reasonable definition is a strictly decreasing function of N_A . We thus turn even more attention to the victim UEs and define a greatly simplified problem

$$\begin{aligned} & \text{minimize} && N_A \\ & \text{subject to} && C_V(N_A) \geq C_{V,\min}, \\ & && 0 \leq N_A \leq N_S. \end{aligned} \quad (54)$$

Now, the throughput of victim UEs depends on quite many things, from which the most important one is how the BS schedules the UEs, i.e., what is the scheduling algorithm and how are victim and non-victim UE transmissions placed in NSFs and ABSFs. In [17] it has been suggested that

proportionally fair scheduler, assuming reliable knowledge of channel state, can take care of the division between NSFs and ABSFs itself. However, scheduling is (and will probably long stay) implementation specific, so that BS hardware and software vendors can compete with each other and fight for the technological edge.

Therefore, to define $C_V(N_A)$, we consider what is from the throughput and scheduling point of view the worst case scenario: average throughput at outage threshold (outage throughput) and round robin scheduling algorithm. Concerning NSF and ABSF division we assume that non-victim UEs have access only to NSFs while victim UEs have access to both NSFs and ABSFs. With these the average victim UE outage throughput is

$$C_V = \mathbb{E}_{L, L_V} \left\{ \frac{N_A}{N_S} C_V^{(A)}(L, L_V) + \frac{N_S - N_A}{N_S} C_V^{(N)}(L, L_V) \right\} \quad (55)$$

where $C_V^{(A)}$ is average victim UE outage throughput in ABSFs, $C_V^{(N)}$ is average victim UE outage throughput in NSFs and L and L_V represent the number of all UEs and the number of victim UEs associated with the BS, respectively. Although L and L_V are correlated, for our purposes the outage throughput C_V can be very well approximated by considering them as independent. We thus write

$$C_V \approx \frac{N_A}{N_S} C_V^{(A)}(L_V) + \frac{N_S - N_A}{N_S} C_V^{(N)}(L). \quad (56)$$

Now, assuming channel independence across resource blocks and using the success probabilities derived in Section III, we can approximate $C_V^{(A)}$ and $C_V^{(N)}$ as

$$C_V^{(A)}(L_V) \approx N_R \mathbb{P} \{ \gamma^{(A)} > \gamma_0 \} \log(1 + \gamma_0) \bar{\Omega}^{(A)}, \quad (57)$$

$$C_V^{(N)}(L) \approx N_R \mathbb{P} \{ \gamma^{(N)} > \gamma_0 \} \log(1 + \gamma_0) \bar{\Omega}^{(N)}, \quad (58)$$

where N_R is number of resource blocks, the $\bar{\Omega}^{(A)}$ and $\bar{\Omega}^{(N)}$ terms denote the average asymptotic proportion of resources that a victim UE is scheduled via the round robin principle in ABSF and NSF, respectively, and $\gamma^{(A)}$ and $\gamma^{(N)}$ denote SIR in ABSF and NSF, respectively. In place of the success probabilities we use the corresponding macro/femto and macro/pico derived terms (30) and (45), respectively. The $\bar{\Omega}^{(A)}$ and $\bar{\Omega}^{(N)}$ values depend on the average number of victim and non-victim UEs per BS. Derivation of these values is presented in the Appendix. Finally, we connect all the acquired results and construct a condition for the number of ABSFs as

$$N_A = \min \left[\left[\frac{N_S (C_{V,\min} - C_V^{(N)})}{C_V^{(A)} - C_V^{(N)}} \right] ; N_S \right]. \quad (59)$$

Table I
REFERENCE SIMULATION PARAMETERS

Parameter	Value
Simulated area	10000m × 10000m
Samples collected from	3000m × 3000m
Macro BS intensity λ_M	10^{-5}m^{-2}
Femto BS intensity λ_F	$12\lambda_M$
Pico BS intensity λ_P	$4\lambda_M$
Macro UE intensity λ_{MUE}	$20\lambda_M$
Macro BS transmission power P_M	43dBm
Femto BS transmission power P_F	20dBm
Pico BS transmission power P_P	30dBm
Macro BS load ϕ_M	1
Femto BS load ϕ_F	0.5
Pico BS load ϕ_P	0.8
MBS-UE path loss exponent α_M	2.5
FBS-UE path loss exponent α_F	3.5
PBS-UE path loss exponent α_P	3
Macro/femto DI-defining k	$\left(\frac{P_F}{P_M}\right)^{\frac{2}{\alpha_M + \alpha_F}} = 0.136$
Macro/pico association bias κ	7dB
Macro/pico association-defining k_1	$\left(\frac{\kappa P_P}{P_M}\right)^{\frac{2}{\alpha_M + \alpha_P}} = 0.471$
Macro/pico DI-defining k_2	$\left(\frac{P_P}{P_M}\right)^{\frac{2}{\alpha_M + \alpha_P}} = 0.262$
ABSf residue interference ρ_A	-20dB
Outage threshold γ_0	-5dB
Number of subframes N_S	10
Number of resource blocks N_R	25
Resource block bandwidth	180kHz

A. Macro/femto scenario

Before moving on to performance evaluation, we demonstrate precision of our outage throughput approximation and analyze dependence of the condition (59) on key parameters. Unless stated otherwise, parameters are at their reference values as shown in Table I. We consider these to be realistic values. Because $\alpha_M \neq \alpha_F$ and $\alpha_M \neq \alpha_P$, we decided to use $(\alpha_M + \alpha_F)/2$ and $(\alpha_M + \alpha_P)/2$ in the definitions of k , k_1 and k_2 . That way we keep the definitions close to the intuitive shape with single α . Impact of different DI-defining coefficients is later considered in the performance evaluation. Unless stated otherwise, the minimum average outage throughput

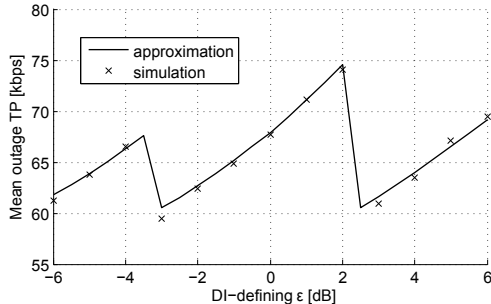


Figure 1. Approximate outage throughput of victim MUEs in macro/femto scenario versus DI definition via ε (as in $k = [P_F / (\varepsilon P_M)]^{2/(\alpha_M + \alpha_F)}$) compared to simulated equivalent.

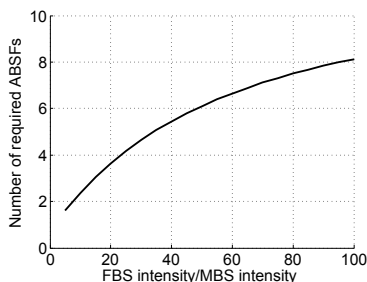


Figure 2. Dependence of required number of ABSFs N_A in macro/femto scenario on FBS intensity λ_F with other parameters constant. The λ_F/λ_M ratio equals mean number of FBSs per MBS coverage.

$C_{V,\min}$ in macro/femto scenario is set to 40kbits/s.

In Fig. 1 we plot the approximation of outage throughput compared to simulated equivalent. Macrocell path loss and minimum average outage throughput are changed from default values to $\alpha_M = 3$ and $C_{V,\min} = 60$ kbits/s in order to increase simulation precision (for further discussion see Section V). Other parameters are at their default values as in Table I. The values of C_V are plotted against definition of DI. The horizontal axis does not present k directly, but a ratio ε that puts into relation own received power and DI received power, i.e., $k = [P_F / (\varepsilon P_M)]^{2/(\alpha_M + \alpha_F)}$. The approximation can be considered very good, with deviations coming mostly from insufficient number of Monte Carlo samples. Within $\varepsilon \in (-4\text{dB}, -3\text{dB})$ and $\varepsilon \in (2\text{dB}, 3\text{dB})$ there is a step in the curve because for given values of k the number of required ABSFs according to our condition (59) changes.

Dependence of (59) on $C_{V,\min}$ and λ_{MUE} is intuitively clear and our results confirm it - the N_A required grows approximately linearly with both of these values. Therefore, we save space and exclude those results. In Fig. 2 we show dependence on λ_F . The trend is approximately linear

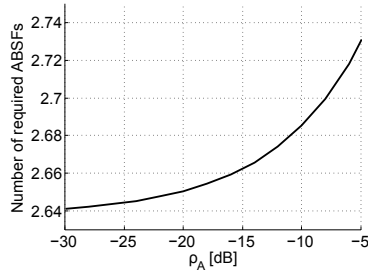


Figure 3. Dependence of the required number of ABSFs N_A in macro/femto scenario on residue ABSF interference ρ_A in macro/femto scenario with other parameters constant.

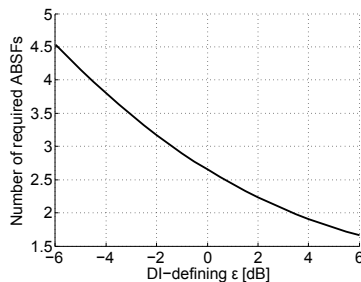


Figure 4. Dependence of the required number of ABSFs N_A in macro/femto scenario on the definition of victim MUE with other parameters constant.

in the beginning and then becomes slightly saturated. In Fig. 3 we show dependence on ρ_A , the residual FBS interference in ABSF. Here the dependence is low because FBS interference is strongly attenuated by larger path loss exponent α_F . Finally in Fig. 4 we show dependence of N_A required on the definition of dominant FBS interferer k via ϵ . With increasing ϵ the k coefficient is decreasing and less MUEs are considered being victim. Although this decreases the N_A required, we are practically increasing the number of non-victim MUEs and therefore have to consider effect on their performance. We will come back to this in Section V.

B. Macro/pico scenario

Similarly to the previous subsection, we present dependence of N_A on selected parameters. The reference parameter values are taken from Table I and the minimum average outage throughput $C_{V,\min}$ is set to 100kbits/s.

In Fig. 5 we show the effect of λ_P value on N_A with other parameters at reference values. Compared to intensity of FBSs in macro/femto scenario, increasing number of PBSs does not primarily increase interference. On the contrary, with higher number of PBSs the MUEs have

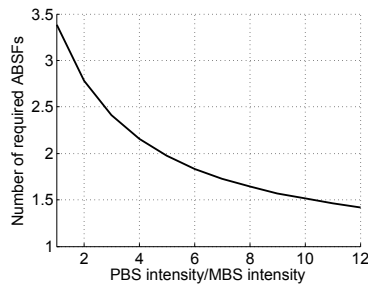


Figure 5. Dependence of the required number of ABSFs N_A in macro/pico scenario on PBS intensity λ_P with other parameters constant. The λ_P/λ_M ratio equals mean number of PBSs per MBS coverage.

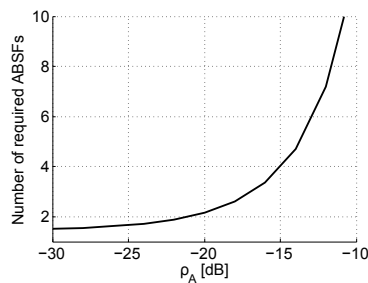


Figure 6. Dependence of the required number of ABSFs N_A in macro/pico scenario on residue ABSF interference ρ_A with other parameters constant.

more BSs to connect to, therefore number of PUEs per PBS decreases and less ABSFs is needed. In Fig. 6 we show dependence of N_A on residue ABSF interference ρ_A . While below $\rho_A = -15$ dB the residue interference seems manageable, higher values leads to dramatic increase in the N_A requirement. The impact is much stronger than in macro/femto scenario. It is partly because of lower path loss exponent on MBS-UE links $\alpha_M < \alpha_F$ and partly because of the vulnerability imposed by the association bias κ . Finally in Fig. 7 we present dependence of N_A on κ . As intuitively expected, increasing κ results in MBS interferers being even closer to the victim PUE and thus the N_A requirement increases.

V. PERFORMANCE ANALYSIS

In this section we demonstrate the effect of the derived number of ABSFs on UE throughput in downlink. We use Monte Carlo simulations to evaluate UE throughput with link adaptation modeled by Shannon's capacity. The simulations consist of snapshots, during which BSs and UEs are dropped and kept at fixed positions, and in each snapshot there are multiple frames (with subframes) where the UEs are scheduled. Reference simulation parameters are summarized

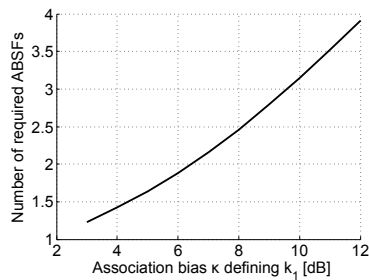


Figure 7. Dependence of the required number of ABSFs N_A in macro/pico scenario on association bias κ , which defines k_1 , with other parameters constant.

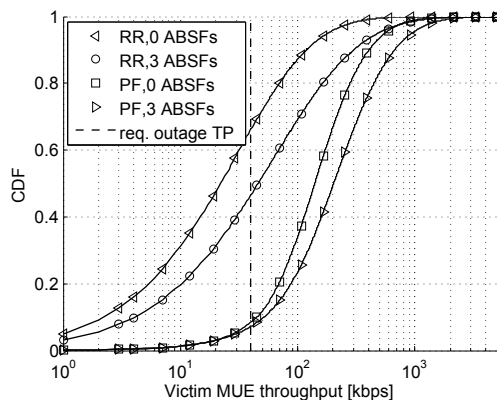


Figure 8. Throughput CDF of victim MUEs in macro/femto scenario with round robin and proportional fair scheduling, with and without ABSFs. The required outage throughput is marked by a dashed line.

in Table I. Although we consider the model parameters realistic, the computational complexity of the simulations prevented us from using a simulated area size that would provide sufficient precision for $\alpha_M = 2.5$. However, rather than using unrealistic parameters we keep the area at manageable value and accept that the performance results in this section are a little on the optimistic side. As a measure of performance we collect aggregate throughput of each MUE/PUE and then evaluate the results in form of UE throughput CDF.

A. Macro/femto scenario

The minimum average outage throughput in macro/femto scenario is set to 40kbps/s. In Fig. 8 we present throughput CDFs of victim MUEs. Victim MUEs are scheduled in both NSFs and ABSFs and for comparison we have included both round robin and proportionally fair scheduling algorithms. The proportionally fair scheduler requires channel knowledge and in each RB it

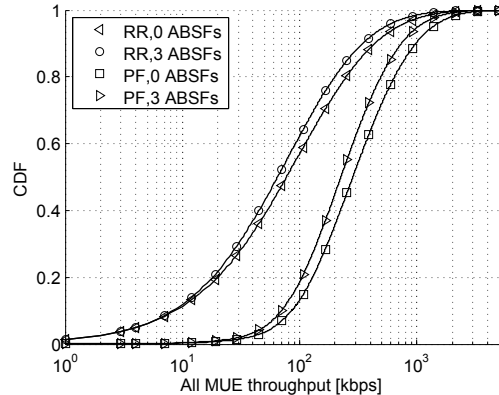


Figure 9. Throughput CDF of all MUEs in macro/femto scenario with round robin and proportional fair scheduling, with and without ABSFs.

chooses the user with highest instantaneous SIR normalized by its mean SIR. The dashed line in Fig. 8 represents the chosen minimum mean victim outage throughput $C_{V,\min}$.

Looking at the victim MUE curves we can observe that in given macro/femto scenario the effect of ABSFs is rather moderate. Without them, around 70% of victim MUEs have lower throughput than $C_{V,\min}$. With ABSFs, approximately 50% have higher throughput than $C_{V,\min}$. With proportionally fair scheduler the throughput values are higher and effect of ABSFs weaker. The large difference between our round robin based requirement and the proportionally fair performance suggests that our research should be expanded by considering advanced scheduling during the ABSF planning phase. The effect of ABSFs on purely non-victim MUEs is not shown, as those obviously lose 30% of available resources. In Fig. 9 we show throughput CDFs of all MUEs combined. The rather small improvement of victim MUE performance seems to be in overall statistics completely overshadowed by the effect of resource restrictions for non-victim users. From the system perspective these findings suggest that rather than blocking femto layer users and non-victim MUEs from a fraction of resources, the MUEs that suffer from strong FBS interference should be treated in an individual manner.

In Fig. 10 we present impact of the DI-defining coefficient k to MUE throughput via the same ε factor as in Subsection IV-A. Because differences in CDF curves are too small to notice with eyes, we put measured mean throughput on the y-axis. In an interval with the same number of ABSFs increasing value of ε leads to less victim and more non-victim MUEs per MBS, therefore victim MUE mean throughput is increasing, while non-victim MUE throughput is decreasing.

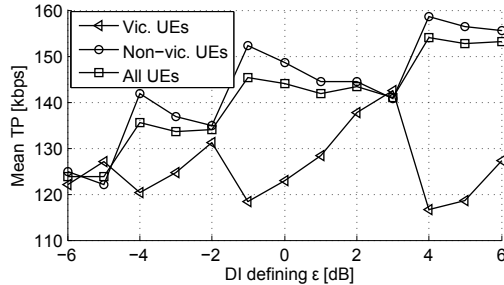


Figure 10. Mean round robin throughput of victim/non-victim/all MUEs in macro/femto scenario versus definition of dominant interferer.

Table II

VICTIM MUE OUTAGE THROUGHPUT AND NON-VICTIM MUE MEAN THROUGHPUT IN KBPS FOR DIFFERENT NUMBERS OF ABSFs IN MACRO/FEMTO SCENARIO.

N_A	1	2	3	4	5
Victim mean outage TP	32	43.6	53.8	65.3	75.4
Non-victim mean TP	188.2	170.7	148.7	128.1	107.7

For our parameters a good point of operation is with $\epsilon \in (2\text{dB}, 3\text{dB})$, where the number of ABSFs is lower than around $\epsilon = -2\text{dB}$ and the mean victim and non-victim MUE throughputs are relatively close to each other.

To justify the simplification of optimization problem (53) into (54) we present in Table II mean outage throughput of victim MUEs and mean throughput of non-victim MUEs for different numbers of ABSFs N_A . Mean throughput of non-victim MUEs is a clearly decreasing function of ABSFs, the simplification is thus well justified. Although the table shows that 2 ABSFs would suffice to fulfill $C_{V,\min} = 40\text{kbps}$ requirement, this is because our simulation area is not large enough as mentioned at the beginning of this section.

B. Macro/pico scenario

In the second scenario we set the $C_{V,\min}$ value to 100kbps/s. In Fig. 11 we present throughput CDFs of victim PUEs with the same round robin and proportionally fair scheduling algorithms. As before, victim PUEs are scheduled in both ABSFs and NSFs, while non-victim PUEs have access only to NSFs. Without ABSFs, the victim PUEs experience very bad performance. Strong cross-layer interference (with $\alpha_M < \alpha_P$) with association bias κ on the top leads to

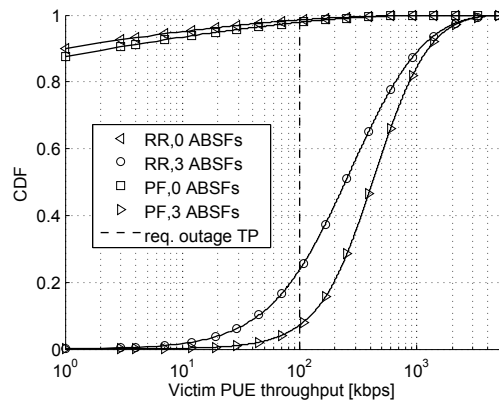


Figure 11. Throughput CDF of victim PUEs in macro/pico scenario with round robin and proportional fair scheduling, with and without ABSFs. The minimum average outage throughput is marked by a dashed line.

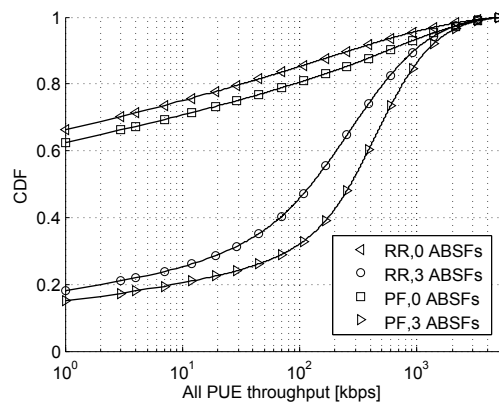


Figure 12. Throughput CDF of all PUEs in macro/pico scenario with round robin and proportional fair scheduling, with and without ABSFs.

very low throughput values. With both round robin and proportionally fair scheduler, more than 95% of victim PUEs experience lower throughput than the $C_{V,\min}$ requirement. With ABSFs, approximately 70% and 90% of victim PUEs reach the requirements using round robin and proportionally fair scheduler, respectively.

In Fig. 12 we plot results from all PUEs. Because of the association bias the proportion of victim PUEs is quite high, therefore the decrease of non-victim PUE performance is not even visible in the figure. Overall, even though there are still PUEs experiencing zero performance, ABSFs substantially improve service in the pico layer. For completeness, Fig. 13 also shows throughput CDFs for all UEs in the scenario, i.e., PUEs as well as MUEs. It confirms that ABSFs are very advantageous for given scenario - high performance gains in the lower percentiles are

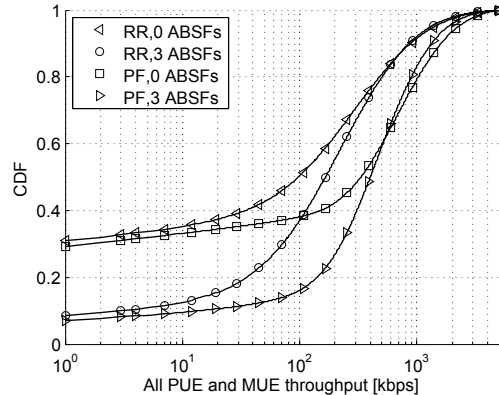


Figure 13. Throughput CDF of all MUEs and PUEs in macro/pico scenario with round robin and proportional fair scheduling, with and without ABSFs.

balanced by relatively small performance decrease in the higher end of the curve.

A sharp reader looking at Fig. 12 and Fig. 13 notices that despite using ABSFs, a percentage of PUEs is experiencing system outage, i.e., no throughput at all. These are PUEs that did not fulfill the DI definition via reference k_2 . To further investigate this important design property we plot in Fig. 14 throughput CDFs of all UEs in macro/pico scenario with multiple values of ε that defines $k_2 = [P_P / (\varepsilon P_M)]^{2/(\alpha_P + \alpha_M)}$. Decreasing the DI definition threshold noticeably increases throughput values in the lower percentiles and thus reduces system outage. Because our reference scenario settings yield relatively low amount of PUEs per PBS, increasing the number of victim PUEs actually does not show any penalty in this result set. This will however not hold in general, as the PBSs are expected to be operational especially in areas with higher UE density.

VI. CONCLUSIONS

Almost blank subframes (ABSFs) offer a simple and efficient way of decreasing the level of background cross-tier interference and thus give an opportunity to serve vulnerable users. We propose a way to approximate the required number of ABSFs based on Poisson point process network deployment statistics. We derive the necessary number of ABSFs as a formula that is easy to evaluate for macro/femto scenario with closed subscriber groups and macro/pico scenario with cell range expansion. We analyze dependence of the result on individual parameters, showing that while in macro/femto scenario the white residue interference in ABSF can be tolerated well, in macro/pico scenario its effect on the required number of ABSFs is substantial. Throughput

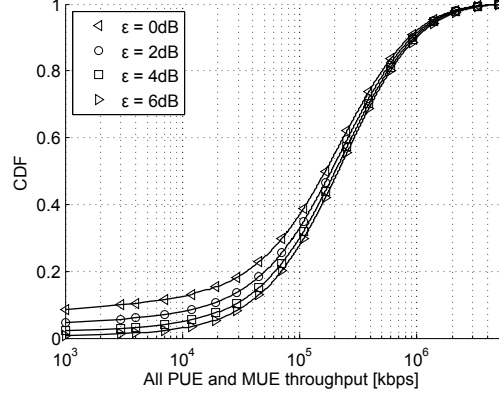


Figure 14. Throughput CDF of all MUEs and PUEs in macro/pico scenario with ABSFs, round robin scheduling and several values of DI-defining k_2 via ε .

$$f_{m/f}^{(N)}(x) \approx \frac{d}{dx} F_S(x, p_{m/f}^{(V)}) = \frac{343e^{-x\left(\frac{7\lambda_M}{2} + S_1\right)} (1 - e^{-xS_1}) \sqrt{\frac{7}{2\pi}} x^{5/2} \lambda_M^{7/2} S_2^3}{5145\sqrt{7}k^6\lambda_F^3\lambda_M^3S_3 + 15435\sqrt{7}k^4\lambda_F^2\lambda_M^4S_3 + 15435\sqrt{7}k^2\lambda_F\lambda_M^5S_3 + 5145\sqrt{7}\lambda_M^6S_3 - S_2^3} \quad (60)$$

$$\bar{\Omega}_{m/f}^{(N)} \approx \frac{\lambda_M^{9/2} \left(\frac{\sqrt{7}}{\lambda_M^{7/2}} - \frac{2401}{S_0^{7/2}} - 2401 \left(\frac{k^2\lambda_F + \lambda_M}{S_2} \right)^{7/2} + 2401 \left(\frac{k^2\lambda_F + \lambda_M}{\lambda_M S_0 + k^2\lambda_F(7\lambda_M + 4\lambda_{MUE})} \right)^{7/2} \right)}{\sqrt{7}\lambda_{MUE} - 16807\lambda_{MUE} \left(\frac{\lambda_M}{7\lambda_M + 2S_1} \right)^{9/2}} \quad (61)$$

$$\bar{\Omega}_{m/f}^{(A)} \approx \frac{1}{\lambda_M} \left(\frac{15\sqrt{2\pi/7}}{343S_4^{7/2}} - \frac{30\sqrt{2\pi}}{(7S_4 + 2\lambda_{MUE})^{7/2}} + \frac{15\sqrt{2\pi}}{(7S_4 + 4\lambda_{MUE})^{7/2}} \right) \left(\frac{15\sqrt{2\pi/7}}{343S_4^{9/2}} - \frac{105\sqrt{2\pi}}{(7S_4 + 2\lambda_{MUE})^{9/2}} \right)^{-1} \quad (62)$$

simulations show that in macro/femto scenario the performance gain when using ABSFs is rather moderate and the system may work better with a more individual treatment of high FBS interference. On the other hand, in the macro/pico scenario we can see that, especially due to the association bias, using ABSFs improves the performance of the system considerably.

The fraction of victim users in outage decreases from over 95% to 30% or even 10%, depending on the scheduling algorithm. Looking at all users in the macro/pico scenario, the small decrease in high throughput percentiles is more than balanced by substantial performance increase in the lower region.

APPENDIX

DERIVATION OF ROUND ROBIN RESOURCE FRACTIONS

If a loaded BS governs L associated UEs and all UEs have uniform traffic requirements, each UE will asymptotically be scheduled in $1/L$ fraction of available resource blocks. We are

interested in expected value of this fraction for victim UEs. Using a clever approach from [35] we can write

$$\bar{\Omega} = C'_\Omega \sum_{\ell=1}^{\infty} \frac{1}{\ell} \mathbb{P} \left\{ \Omega = \frac{1}{\ell} \right\} \quad (63)$$

$$= C'_\Omega \sum_{\ell=1}^{\infty} \frac{1}{\ell} \ell \mathbb{P} \{ L = \ell \} \quad (64)$$

$$= C'_\Omega \sum_{\ell=1}^{\infty} \int_0^{\infty} \mathbb{P} \{ L = \ell | A = x \} f_A(x) dx \quad (65)$$

$$= C'_\Omega \sum_{\ell=1}^{\infty} \int_0^{\infty} \frac{(x \lambda_{\text{MUE}})^\ell}{\ell!} e^{-\lambda_{\text{MUE}} x} f_A(x) dx \quad (66)$$

$$= C'_\Omega \int_0^{\infty} e^{-\lambda_{\text{MUE}} x} f_A(x) \sum_{\ell=1}^{\infty} \frac{(x \lambda_{\text{MUE}})^\ell}{\ell!} dx \quad (67)$$

$$= C'_\Omega \int_0^{\infty} (1 - e^{-\lambda_{\text{MUE}} x}) f_A(x) dx, \quad (68)$$

where $f_A(x)$ is a PDF of an area where the given set of UEs can be located and C'_Ω and C_Ω are normalization constants. We denote the area PDF $f_A(x)$ as $f_{\text{m/f}}^{(N)}(x)$ for all MUEs in macro/femto scenario (round robin fraction in NSF), $f_{\text{m/f}}^{(A)}(x)$ for victim MUEs in macro/femto scenario (round robin fraction in ABSF), $f_{\text{m/p}}^{(N)}(x)$ for all PUEs in macro/pico scenario and $f_{\text{m/p}}^{(A)}(x)$ for victim PUEs in macro/pico scenario. The normalization constant C'_Ω is needed because we are excluding cases with no UEs associated to BS, while C_Ω takes also into account multiplying the PMF $\mathbb{P} \{ L = \ell \}$ with a weight factor ℓ and can be calculated from

$$C_\Omega^{-1} = \sum_{\ell=1}^{\infty} \ell \mathbb{P} \{ L = \ell \} \quad (69)$$

⋮

$$= \int_0^{\infty} \lambda_{\text{MUE}} x f_A(x) dx. \quad (70)$$

In macro/femto scenario the PDF $f_{\text{m/f}}^{(N)}(x)$ can be obtained from the general approximation of a Poisson Voronoi cell area that has been found in [36] (and used in [35]) by adding a condition that there is at least one victim MUE present. The general Voronoi area for our macro PPP is drawn from PDF

$$f_S(x) \approx \lambda_M \frac{343}{15} \sqrt{\frac{7}{2\pi}} (\lambda_M x)^{\frac{5}{2}} \exp \left(-\frac{7}{2} \lambda_M x \right). \quad (71)$$

The PDF $f_{m/f}^{(N)}(x)$ can be obtained from CDF

$$F_S(x, p^{(V)}) = \mathbb{P} \{ S \leq x | L_V > 0 \} \quad (72)$$

$$= \frac{\mathbb{P} \{ S \leq x, L_V > 0 \}}{\mathbb{P} \{ L_V > 0 \}} \quad (73)$$

$$= \frac{\int_0^x \mathbb{P} \{ L_V > 0 | S = u \} f_S(u) du}{\int_0^\infty \mathbb{P} \{ L_V > 0 | S = u \} f_S(x) dx} \quad (74)$$

$$= \frac{\int_0^x (1 - \mathbb{P} \{ L_V = 0 | S = u \}) f_S(u) du}{\int_0^\infty (1 - \mathbb{P} \{ L_V = 0 | S = u \}) f_S(x) dx} \quad (75)$$

$$= \frac{\int_0^x \left(1 - e^{-p^{(V)} \lambda_{MUE} u} \right) f_S(u) du}{\int_0^\infty \left(1 - e^{-p^{(V)} \lambda_{MUE} x} \right) f_S(x) dx}, \quad (76)$$

where $p^{(V)}$ is a probability that a UE is a victim UE, i.e., in macro/femto scenario $p_{m/f}^{(V)} = \mathbb{P} \left\{ N_{DI}^{(F)} \geq 1 \right\}$ from (28). After calculating the integrals in (76) and differentiating the CDF we get a result (60) with subterms:

$$S_0 = 7\lambda_M + 2\lambda_{MUE} \quad (77)$$

$$S_1 = \frac{k^2 \lambda_F \lambda_{MUE}}{k^2 \lambda_F + \lambda_M} \quad (78)$$

$$S_2 = (7\lambda_M^2 + k^2 \lambda_F S_0) \quad (79)$$

$$S_3 = \sqrt{\frac{\lambda_M (k^2 \lambda_F + \lambda_M)}{7\lambda_M^2 + k^2 \lambda_F S_0}} \quad (80)$$

The PDF $f_{m/f}^{(A)}(x)$ of area where victim MUEs can be located is not trivial to find. The most sensible approach we came up with is transforming the unconditional Voronoi cell random variable using again the probability that MUE is a victim MUE, i.e.,

$$f_{m/f}^{(A)}(x) = \frac{1}{p_{m/f}^{(V)}} f_{m/f}^{(N)} \left(\frac{x}{p_{m/f}^{(V)}} \right). \quad (81)$$

In macro/pico scenario the pdf of area of all UEs within a macrocell conditioned on presence of a victim PUE is

$$f_{m/p}(x) = \frac{d}{dx} F_S(x, p_{m/p}^{(V)}), \quad (82)$$

where $p_{m/p}^{(V)} = \mathbb{P} \{ k_2 r_M < r_P < k_1 r_M \}$ as in (43). For PUEs and victim PUEs we make a similar approximation as in (81) with addition of further multiplying the transformation coefficients with

the average number of PBSs within MBS coverage, resulting in

$$f_{m/p}^{(N)}(x) = \frac{\lambda_M}{\lambda_P} \frac{1}{\mathbb{P}\{r_P < k_1 r_M\}} \times f_{m/p} \left(\frac{\lambda_M}{\lambda_P} \frac{x}{\mathbb{P}\{r_P < k_1 r_M\}} \right), \quad (83)$$

where

$$\mathbb{P}\{r_P < k_1 r_M\} = \frac{k_1^2 \lambda_P}{k_1^2 \lambda_P + \lambda_M} \quad (84)$$

and

$$f_{m/p}^{(A)}(x) = \frac{\lambda_M}{\lambda_P} \frac{1}{p_{m/p}^{(V)}} f_{m/p} \left(\frac{\lambda_M}{\lambda_P} \frac{x}{p_{m/p}^{(V)}} \right). \quad (85)$$

The round robin fraction values $\bar{\Omega}$ can be obtained in closed form for all cases. For macro/femto scenario we present them in (61) and (62) with subterms given here:

$$S_4 = \lambda_M \left(1 + \frac{\lambda_M}{k^2 \lambda_F} \right) \quad (86)$$

Formulas for $f_{m/p}^{(N)}(x)$, $f_{m/p}^{(A)}(x)$, $\bar{\Omega}_{m/p}^{(N)}$ and $\bar{\Omega}_{m/p}^{(A)}$ we leave out of the paper because they are very spacious and do not have enough added value by themselves. To illustrate the precision of our approximations we show the $\bar{\Omega}$ values as functions of λ_{MUE}/λ_M in Fig. 15. The approximation of $\bar{\Omega}_{m/f}^{(N)}$ is very good. In other cases our derived formulas give consistently lower values than the simulations. The reason behind this is that when transforming the Voronoi area PDFs $f_{m/f}(x)$ and $f_{m/p}(x)$ we neglect that dangerous zones around FBSs and coverage areas of PBSs can overlap. Nevertheless, the derived values $\bar{\Omega}_{m/f}^{(A)}$, $\bar{\Omega}_{m/p}^{(N)}$ and $\bar{\Omega}_{m/p}^{(A)}$ serve as a good lower bound and ensure that the required number of ABSFs as given in Section IV will not be too low.

REFERENCES

- [1] 3GPP, "Evolved Universal Terrestrial Radio Access (E-UTRA) and Evolved Universal Terrestrial Radio Access Network (E-UTRAN); Overall description; Stage 2," 3GPP tech. spec. TS 36.300, Ver. 10.8.0, July 2012
- [2] R1-104968, "Summary of the description of candidate eICIC solutions," Contribution at 3GPP meeting in Madrid, Spain, August 2010
- [3] D. Lopez-Perez, I. Guvenc, G. de la Roche, M. Kountouris, T.Q.S. Quek, J. Zhang, "Enhanced Intercell Interference Coordination Challenges in Heterogeneous Networks," *IEEE Wireless Commun.*, vol.18, no.3, pp.22-30, June 2011
- [4] X. Li, L. Qian, D. Kataria, "Downlink Power Control in Co-Channel Macrocell Femtocell Overlay," *43rd Ann. Conf. on Information Sciences and Systems, 2009 (CISS 2009)*, pp.383-388, 18-20 March 2009
- [5] D. Lopez-Perez, A. Valcarce, G. de la Roche, Jie Zhang, "OFDMA femtocells: A roadmap on Interference Avoidance," *IEEE Commun. Mag.*, vol.47, no.9, pp.41-48, September 2009

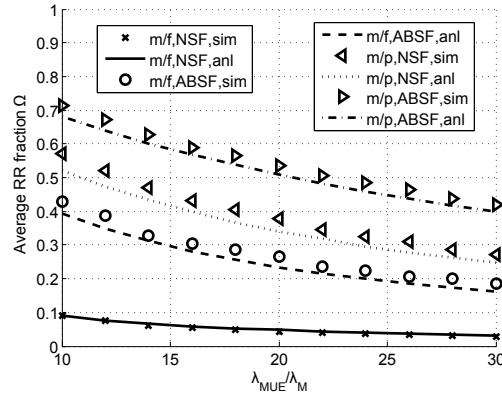


Figure 15. Average round robin fraction $\bar{\Omega}$ in macro/femto (m/f) and macro/pico (m/p) scenario. Markers represent simulated values, lines represent analytically approximated values.

- [6] Z. Bharucha, A. Saul, G. Auer, H. Haas, "Dynamic Resource Partitioning for Downlink Femto-to-Macro-Cell Interference Avoidance," *EURASIP Journal on Wireless Commun. and Networking*, vol. 2010, Article ID 143413, 12 pages, 2010
- [7] A. Elsherif, A. Ahmedin, Z. Ding, X. Liu, "Adaptive Precoding for Femtocell Interference Mitigation," *2012 IEEE Int. Conf. on Commun. (ICC)*, 10-15 June 2012
- [8] S.-Y. Lien, C.-C. Tseng, K.-C. Chen, C.-W. Su, "Cognitive Radio Resource Management for QoS Guarantees in Autonomous Femtocell Networks," *2010 IEEE Int. Conf. on Commun. (ICC)*, 23-27 May 2010
- [9] A. Elsherif, A. Ahmedin, Z. Ding, X. Liu, J. Hämäläinen, R. Wichman, "Shadow Chasing: A Resource Allocation Scheme for Heterogeneous Networks," *IEEE 7th Int. Conf. on Cognitive Radio Oriented Wireless Networks*, July 2012
- [10] R1-083813, "Range expansion for efficient support of heterogeneous networks," Contribution at 3GPP meeting in Prague, Czech Republic, September 2008
- [11] R. Wang, Y. Du, "Het-Net Throughput Analysis with Picocell Interference Cancellation," *2011 IEEE Int. Conf. on Commun. Workshops (ICC)*, 5-9 June 2011
- [12] C.-H. Huang, C.-Y. Liao, "An Interference Management Scheme for Heterogeneous Network with Cell Range Extension," *2011 13th Asia-Pacific Network Operations and Management Symp. (APNOMS)*, 21-23 September 2011
- [13] D. Lopez-Perez, X. Chu, "Inter-Cell Interference Coordination for Expanded Region Picocells in Heterogeneous Networks," *2011 Proc. of 20th Int. Conf. on Comput. Commun. and Networks (ICCCN)*, July 2011
- [14] M. Huang, W. Xu, "Macro-Femto Inter-Cell Interference Mitigation for 3GPP LTE-A Downlink," *2012 IEEE Wireless Commun. and Networking Conf. Workshops (WCNCW)*, pp.75-80, April 2012
- [15] A. Damnjanovic, J. Montojo, J. Cho, H. Ji, J. Yang, P. Zong, "UE's Role in LTE Advanced Heterogeneous Networks," *IEEE Commun. Mag.*, vol.50, no.2, pp.164-176, February 2012
- [16] S. Hämäläinen, H. Sanneck, C. Sartori, "LTE Self-Organising Networks (SON): Network Management Automation for Operational Efficiency," John Wiley & Sons, 2012
- [17] Y. Wang, K. I. Pedersen, "Time and Power Domain Interference Management for LTE Networks with Macro-Cells and HeNBs," *2011 IEEE Veh. Technology Conf. (VTC Fall)*, 5-8 Sept. 2011
- [18] A. Ghosh, N. Mangalvedhe, R. Ratasuk, B. Mondal, M. Cudak, E. Visotsky, T.A. Thomas, J.G. Andrews, P. Xia, H.S. Jo, H.S. Dhillon, T.D. Novlan, "Heterogeneous Cellular Networks: From Theory to Practice," *IEEE Commun. Mag.*, vol.50, no.6, pp.54-64, June 2012

- [19] M. Kamel, K. Elsayed, "Performance Evaluation of a Coordinated Time-Domain eICIC Framework based on ABSF in Heterogeneous LTE-Advanced Networks," *IEEE Globecom 2012*
- [20] K. Okino, T. Nakayama, C. Yamazaki, H. Sato, Y. Kusano, "Pico Cell Range Expansion with Interference Mitigation toward LTE-Advanced Heterogeneous Networks," *2011 IEEE Int. Conf. on Commun. Workshops (ICC)*, 5-9 June 2011
- [21] I. Guvenc, "Capacity and Fairness Analysis of Heterogeneous Networks with Range Expansion and Interference Coordination," *IEEE Commun. Lett.*, vol.15, no.10, pp.1084-1087, October 2011
- [22] S. Singh, J.G. Andrews, "Joint Resource Partitioning and Offloading in Heterogeneous Cellular Networks," available at <http://arxiv.org/abs/1303.7039>
- [23] D. Stoyan, W.S. Kendall, J. Mecke, "Stochastic Geometry and its Applications, 2nd Edition," Wiley, 1996
- [24] F. Baccelli, B. Blaszczyszyn, P. Muhlethaler, "Stochastic Analysis of Spatial and Opportunistic Aloha," *IEEE J. Sel. Areas Commun.*, vol.27, no.7, pp.1105-1119, September 2009
- [25] J.G. Andrews, F. Baccelli, R.K. Ganti, "A Tractable Approach to Coverage and Rate in Cellular Networks," *IEEE Trans. Commun.*, vol.59, no.11, pp.3122-3134, November 2011
- [26] D.B. Taylor, H.S. Dhillon, T.D. Novlan, J.G. Andrews, "Pairwise Interaction Processes for Modeling Cellular Network Topology," *IEEE Globecom 2012*
- [27] W.C. Cheung, T.Q.S. Quek, M. Kountouris, "Throughput Optimization, Spectrum Allocation, and Access Control in Two-Tier Femtocell Networks," *IEEE J. Sel. Areas Commun.*, vol.30, no.3, pp.561-574, April 2012
- [28] S. Mukherjee, "Distribution of Downlink SINR in Heterogeneous Cellular Networks," *IEEE J. Sel. Areas Commun.*, vol.30, no.3, pp.575-585, April 2012
- [29] H.S. Dhillon, R.K. Ganti, J.G. Andrews, "Load-Aware Modeling and Analysis of Heterogeneous Cellular Networks," available at <http://arxiv.org/abs/1204.1091>
- [30] I. Guvenc, M.-R. Jeong, F. Watanabe, H. Inamura, "A Hybrid Frequency Assignment for Femtocells and Coverage Area Analysis for Co-Channel Operation," *IEEE Commun. Lett.*, vol.12, no.12, pp.880-882, December 2008
- [31] S. Singh, H.S. Dhillon, J.G. Andrews, "Offloading in Heterogeneous Networks: Modeling, Analysis, and Design Insights," available at <http://arxiv.org/abs/1208.1977>
- [32] H.S. Dhillon, R.K. Ganti, F. Baccelli, J.G. Andrews, "Modeling and Analysis of K-Tier Downlink Heterogeneous Cellular Networks," *IEEE J. Sel. Areas Commun.*, vol.30, no.3, pp.550-560, April 2012
- [33] H.-S. Jo, Y.J. Sang, P. Xia, J.G. Andrews, "Outage Probability for Heterogeneous Cellular Networks with Biased Cell Association," *2011 IEEE Global Telecommun. Conf. (GLOBECOM 2011)*, 5-9 December 2011
- [34] S. Mukherjee, "Downlink SINR distribution in a Heterogeneous Cellular Wireless Network with Biased Cell Association," *2012 IEEE Int. Conf. on Commun. (ICC)*, pp.6780-6786, 10-15 June 2012
- [35] S.M. Yu and S.-L. Kim, "Downlink Capacity and Base Station Density in Cellular Networks," available at <http://arxiv.org/abs/1109.2992>
- [36] J.-S. Ferenc, Z. Néda, "On the size distribution of Poisson Voronoi cells," *Physica A: Statistical Mechanics and its Applications*, Volume 385, Issue 2, 15 November 2007, Pages 518-526